AFM and electron microscopy study of the unusual aggregation behavior of metallosurfactants based on iron(II) complexes with bipyridine ligands.

Paula Garcia,[a] *Peter Eaton,*[a] *Huub P. M. Geurts,*[b] *Miguel Sousa,*[a] *Paula Gameiro,*[a] *Martin C. Feiters,*[*c] *Roeland J. M. Nolte,*[c] *Eulália Pereira,*[*a] *and Baltazar de Castro.*[a]

a REQUIMTE/Departamento de Química, Faculdade de Ciências, Universidade do Porto, Rua do Campo Alegre, 687, 4169-007 Porto, Portugal. Fax: +351 22 6082 959; Tel: +351 22 6082 888; Email: efpereir@fc.up.pt

b Central Facility for Electron Microscopy, Department of General Instrumentation, Radboud University Nijmegen, Toernooiveld, NL-6525 ED Nijmegen, The Netherlands.

c Department of Organic Chemistry, Institute for Molecules and Materials, Radboud University Nijmegen, Toernooiveld, NL-6525 ED Nijmegen, The Netherlands. Fax: +31 24 365 2929; Tel: + 31243652016; E-mail: m.feiters@science.ru.nl

The aggregation behavior in water of three iron (II) complexes with alkylated derivatives of 2,2'-bipyridine was studied by electron microscopy (SEM, cryo-SEM, TEM) and AFM. The results show that minor changes in the length of the ligand alkyl

chains induce remarkable changes in the morphology of the self-assembled aggregates in aqueous solution, *viz.* from rod-like to spherical aggregates.

Introduction

The attachment of lipophilic carbon chains to ligands followed by complexation with transition metals provides a means of combining amphiphilic properties, such as surface activity and self assembly, with the physicochemical properties of metal complexes, namely rich spectroscopic properties, acid-base and redox activity, magnetic properties, etc. Several applications have been proposed for metallosurfactants such as use as probes for magnetic resonance imaging,[1] templates for mesoporous materials,[2, 3] metallomesogens,[4, 5] sensitizers for optoelectronic devices, [6-10] homogeneous catalysts,[11-13] and as antihelmintic therapeutics.[14] The affinity of transition metal ions for certain amphiphilic chelating compounds has also been used to promote vesicle formation,[15, 16] and layer-by-layer film formation.[17] In particular, lipophilic derivatives of 2,2'-bipyridine have been widely used to confer amphiphilic properties on metal complexes,[2, 3, 6, 7, 9, 10, 18-24] with possible catalytic and photophysical applications. Nevertheless, the aggregation behavior of bipyridine-based metallosurfactants is still poorly explored. Many of the studies in the literature report the formation of micelles from metallosurfactants in solution,[25-28] although evidence for inverted vesicles has also been reported.[22]

In order to evaluate the ability of lipophilic derivatives of 2,2'-bipyridine as building blocks for metal-containing nanoassemblies we have synthesized and studied the aggregation behavior in water of the complexes $[FeL_2(CN)_2]$ **1-5** (**1**, L= 4,4'-dipentyl-2,2'-bipyridine; **2**, L= 4,4'-diheptyl-2,2'-bipyridine; **3**, L= 4-heptyl-4'methyl-2,2'-bipyridine; **4**, L= 4,4'-dinonyl-2,2'-bipyridine, **5**, L= 4,4'-bis(tridecyl)-2,2'-bipyridine; Scheme 1). Aggregation of complexes **1-5** was first detected in water-methanol, water-

acetone and water-acetonitrile solutions, where a sharp decrease in λ_{max} of the MLCT band in conjunction with an increase in light scattering was observed for water-rich solutions.[29] These complexes are known to be strongly solvatochromic, and the spectral changes observed can be related to the existence of a lipophilic microenvironment around the metal center.[29, 30] The lipophilic micro-environment is a strong indication that the compounds aggregate in water-rich solutions. In all cases, these aggregates were stable for at least several months without any evidence of precipitation. In a preliminary communication we reported the results obtained by TEM and dynamic light-scattering for compound **4**, that revealed the formation of spherical aggregates with diameters ranging from 200-500 nm.[19]

In the present paper we report a TEM, SEM and AFM study on the morphology of the aggregates of the complexes $[FeL_2(CN)_2]$ **1-5**, in water and in water-methanol mixtures.

Experimental

The complexes were prepared using a published procedure with minor modifications, [19, 29, 31] affording **1-5** in the *cis*-configuration. The aggregates were obtained by injecting 50 μL of a methanol solution of the desired compound (10^{-3} M) into 10 mL of an aqueous solution at 65 ºC, under Ar bubbling. After injection, the solution was maintained at 65 ºC for at least 5 min with Ar bubbling for organic solvent elimination. TEM was carried out in a JEOL-TEM 1010 microscope, operating at 60 KeV, on samples dried on formvar-coated copper grids (200 mesh), without the addition of contrast agent, since the presence of the metal ion provides enough contrast. SEM was carried out in a JEOL FEG-SEM (JSM-6330F) microscope, operating at 3 KeV, WD=8 mm, on samples dried on glass slides coated with Au/Pd by sputtering. Cryo-SEM was carried out on the same instrument used for conventional SEM with an Oxford Cryo transfer system CT1500 HF; the sample was rapidly frozen in nitrogen slush at -220 ºC,

fractured in the cooling pre-chamber of the microscope at -120 °C, subjected to Au/Pd sputtering (1.5 nm), and transferred to the microscope chamber, where it was kept at -120 °C. Samples were prepared for AFM by depositing the vesicles onto freshly cleaved mica sheets, followed by drying, either under ambient conditions, or by extended vacuum drying followed by storage in the vacuum desiccator. All solutions for AFM were prepared using ultrapure pre-filtered water (18MΩ water for molecular biology, Sigma), to avoid contamination. Samples were examined using a Molecular Imaging PicoLE atomic force microscope in tapping mode. Rectangular silicon cantilevers of resonant frequency of 75-155kHz and nominal tip radius <10nm (MikroMasch, Tallinn, Estonia) were used.

Results

Electron microscopy study of freshly prepared samples. The compounds studied are insoluble in water, even at high temperature, with stirring and sonication. Nevertheless, stable colloidal solutions are obtained by addition of water to a methanol solution of the compound or by injection of a small volume of a methanol solution of the desired compound, into water at 65 °C, with stirring and under argon. This injection method is commonly used in the preparation of phospholipid vesicles.[32, 33] Formation of aggregates was immediately perceived by a color change from red (monomer) to blue (aggregates).

The morphological properties of the aggregates formed by the present complexes were studied by SEM, TEM, and cryo-SEM. In all cases, the results obtained by the three techniques were similar, which shows that the aggregates observed by SEM and TEM are present in solution, and no drying artifacts were observed by these techniques. SEM images of freshly prepared samples of the complexes studied are shown in Figure 1. The length of the alkyl chains in 2,2'-bipyridine seems to be a key structural factor for

the morphology of the aggregates. Compound **1** (Figure 1A), with four 5-carbon chains, formed rod-like aggregates with average lengths that varied considerably from sample to sample, *viz.* from 650 to 3500 nm and widths that varied within the range 60-150 nm. Cryo-SEM images showed the same type of rod-like aggregates, some of them protruding from the surface (Figure 2A, black arrows). In addition to the rod-like structures, cryo-SEM images showed some large sheet-like aggregates (Figure 2A, grey arrow) and some disrupted films lying on the surface (Figure 2A, white arrow), possibly resulting from compound that remained after solvent evaporation.

SEM images for compound **2** (Figure 1B) with four 7-carbon chains also showed rod-like aggregates, although with lower average aspect ratio (length range 65-430 nm, width range 45-170 nm), as well as spherical aggregates (diameter range 20-220 nm). In this case, the individual structures were clustered in a three-dimensional network both in frozen solution (cryo-SEM, Figure 2B) and in dehydrated samples (SEM, Figure 1B).

Compound **3**, with one 7-carbon chain and one methyl group on each ligand, (Figure 1C) showed a homogeneous population of elongated aggregates, but in this case the structures are wider in the middle than at the ends, resembling rice-grains (length range 65-430 nm; range of widths at the middle 40-170 nm).

Compound **4,** (Figure 1D, 2C), with four 9-carbon chains, showed only spherical aggregates with diameters in the range of 30-270 nm. These aggregates were partially clustered in the SEM samples probably due to the dehydrating conditions of the sample, since in freshly prepared frozen samples studied by cryo-SEM no clusters were observed.

Compound **5** showed only spherical aggregates, but two different populations were observed: aggregates with diameters in the range of 5-10 nm (Figure 1E, inset) and aggregates with a mean diameter of ≈ 120 nm (Fig 1 E).

Except for the 5-10 nm aggregates observed for **5**, all the other aggregates detected have dimensions that exclude the possibility of micellar structures, since such structures usually have radii of the order of magnitude of the length of the extended molecule.[33, 34] The range of sizes observed is typical for vesicle-like aggregates. This means that they should have an aqueous core, which can be easily detected by simple encapsulation experiments using a strongly hydrophilic fluorescent probe, such as 5(6)-carboxyfluorescein.[33] This assay is commonly used to probe the formation of vesicles in phospholipid suspensions, and is based on the strong auto-quenching effect of the probe. Samples were prepared as usual, but using a 1 M aqueous solution of 5(6)-carboxyfluorescein instead of pure water. At this concentration, fluorescence of the probe is low due to auto-quenching. After checking the formation of the aggregates by UV/vis spectroscopy, the aggregates were separated from free probe by size exclusion chromatography (Sephadex G50). The presence of an aqueous core in the aggregates may be ascertained by checking the fluorescence intensity of the sample after separation, with and without addition of a vesicle disruption agent, *e.g.* Triton X100. If the fluorescence intensity increases drastically after the addition of Triton X100, then an aqueous core must have been present in the aggregates, since the addition of Triton X100 releases the fluorescent probe to the bulk solution, decreasing its concentration and thus the auto-quenching effect. For all the complexes studied, a strong increase in fluorescence was observed after adding Triton X100 (increase of 2-20 times), showing that the hydrophilic probe remained trapped inside an aqueous core. It should be noted that for compound **5**, like for the other complexes, only one fraction was detected that displayed fluorescence after treatment with Triton X100, in spite of the observation by microscopy of two different populations of very different size. Since the elution

volumes of the fractions for compounds **4** and **5** were very similar, the fluorescent fraction for compound **5** was ascribed to the 120 nm aggregates.

Electron microscopy study of aged samples. In all cases, the individual aggregates, once formed, showed a strong tendency towards clustering or fusion in solution at room temperature, and after a few days at room temperature, larger fused or clustered structures were observed, depending on the complex. Fusion was the main process for compound **1** while clustering seemed to be the prevailing process for all the other compounds studied. Figure 3A shows an SEM image obtained for a sample of compound **1**, 1 day after preparation. The morphology of the aggregates in the sample is similar to that observed for freshly prepared samples, but there is a marked increase in the average length and in the average width, showing that fusion is a non-directional process. In contrast, compounds **2** and **4** displayed mainly clustering of the formed aggregates. Cryo-SEM images of samples of compound **2**, 9 days after preparation, showed the formation of micro-domains formed by aggregation of rod-like structures (Figure 3B, 3C), that in some cases were surrounded by a film. Some of these latter structures were broken (probably as a result from the cryo-fracturing of the samples) showing a core containing rod-like aggregates (Figure 3C). In both types of structures the individual rod-like aggregates showed a marked increase in their length (length determined by SEM of 200 nm - 1 μm), indicating that fusion also contributed to the ageing process of the aggregates. Studies on aged samples of compound **4** showed that the formation of clusters of spherical particles was a faster process, and after 1 day in solution the majority of the spherical aggregates had become clustered in solution. After 9 days in solution the only structures detected by cryo-SEM (Figure 3D) were microdomains with average length of ≈ 4 μm surrounded by a film. Some of these

spherical or oval-shape micro-domains were broken and revealed a core made up of individual spherical aggregates.

Effect of incubation time and solvent. The incubation time at 65 ºC and the amount of methanol are also important factors that influence the properties of the aggregates. SEM images of samples prepared by the same method at room temperature and at 65 ºC but limiting the incubation period at the latter temperature to less than 2 min, showed only irregular structures with diameters of 100-200 nm for all the compounds studied. For incubation periods at 65 ºC of 5-15 min formation of rod-like structures was observed for **1**, **2**, and **3**, while for the other compounds studied the aggregates maintained their spherical morphology but became much more regular and attained smoother surfaces. For the compounds that formed rod-like structures the average length of the rods increased with the incubation time. For the 15 min incubation samples some clustering of the structures was detected, but for longer incubation periods the number of aggregates detected in the sample decreased and most of the sample was composed of irregular films.

The effect of adding methanol was studied for methanol concentrations of 0.5-25 % (v:v). The addition of this solvent was done both before and after incubation at high temperature, and the results were similar. For all the compounds studied, increasing amounts of methanol caused a decrease of the stability of the aggregates relative to the dehydrating conditions of the SEM experiments. Figure 4A shows a typical picture of a sample of **1** containing 5 % of methanol, where clearly some of the aggregates are partially collapsed. For larger amounts of methanol more collapsed structures were observed. In addition, the remaining aggregates showed an irregular surface, in contrast to what was observed in water where all the aggregates showed a smooth surface. With 10-75 % methanol present in solution, the samples in all cases showed large round films

with average diameters of 2-5 μm (Figure 4B). These films showed a darker exterior boundary, indicating that they were probably formed by the collapse of large vesicle-type structures. Similar structures were also seen for those compounds that formed rod-like aggregates in water. The amount of methanol necessary to induce these changes was found to be lower for the longer alkyl chain samples. For example, complex **4** in methanol/water 1% v:v (or higher amounts of methanol) formed mainly large vesicles with diameters of 0.5-3 μm, in agreement with our previously reported TEM images.[19]

AFM study. In order to gain insight into the 3-dimensional structure of the aggregates, atomic force microscopy was carried out. Compounds **1** and **4** were selected for this study because they were representative of the different morphologies observed (i.e. rod-like and spherical, respectively). AFM images of aggregates prepared from compounds **1** and **4** are shown in Figure 5A and 5C, respectively. Both samples were dried under ambient conditions. The structures of the aggregates were quite similar to those observed by SEM and TEM. Table 1 shows that the dimensions of the aggregates as measured by the TEM, SEM, and AFM techniques are quite similar, although the variation between batches was quite large. In general, the height as measured by AFM was somewhat smaller than the width as measured by TEM or SEM. TEM shadowing experiments (not shown) showed that the rod width and rod heights were the same for individual rods. Quantitative measurement of the width of such high-aspect ratio features by AFM is not possible, however, due to convolution of the sample topography with the shape of the tip.[35]

In some, but not all cases, further dehydration of the samples of **1** and **4** by vacuum desiccation led to aggregates with a considerably different morphology. Two such images of dehydrated aggregates are shown in Figures 5B (compound **1**) and 5D (compound **4**). Figure 5B shows the typical rods of the pentyl modified compound, but

with a distinctive "flattened" morphology. In addition, the rods are surrounded by some collapsed material. This effect was seen several times for dehydrated aggregates, although it did not always occur. In addition, it was possible to observe intact aggregates, as well as flattened aggregates in the same sample. However, this flattened morphology was never seen unless the samples had been vacuum dried. Figure 5D shows that the aggregates of compound **4** were also strongly affected by drying. These vacuum-dried aggregates appeared broader and flatter than those dried under ambient conditions (5C). Furthermore each aggregate was surrounded by a broad plateau, which was 2.6 nm (standard deviation 0.2 nm) high. Again, this effect was only seen for some aggregates after vacuum drying, but never for aggregates prepared under ambient conditions.

Discussion

The aggregation behavior observed for the compounds studied in this work is typically that of amphiphilic molecules, containing a hydrophilic headgroup and a hydrophobic tail. These molecules form self-assembled structures in water, in order to maximize the interactions of the hydrophilic part with the solvent, while minimizing the contact of the hydrophobic part with the solvent. In the case of compounds **1**-**5**, **t**he alkyl chains are obviously hydrophobic, as are also probably the bipyridine ligands,[36] which can also interact with each other by π- π stacking. The known solvatochromism of $[Fe(bpy)_2(CN)_2]$ and related alkyl-substituted species, which is the result of hydrogen bonding of the cyanide ligands to protic solvents,[29, 30] is evidence of the hydrophilicity of the highly polar $Fe(II)(CN)_2$ moiety in the complexes **1-5** despite the fact that this moiety has no net charge and does not dissociate in ions. The absence of any charge repulsion combined with the overall high hydrophobicity, including both the alkyl and

bipyridine moieties explains the self-assembly in water of compounds **1-3**, despite the fact that they contain only short alkyl tails. Nevertheless, it should be noted that the difference in lipophilicity between **1**, and the same compound with 4-methyl-4'-pentyl-2,2'-bipyridine ligands is sufficient to make the latter compound water soluble.[30]

In order to understand the self-assembly behavior of the present compounds, it is useful to compare their structural features and behavior with those of previously reported ruthenium complexes of general formula $[Ru(bpy)_2(4,4'\text{-}R_2bpy)]^{2+}$, where R is 12 or 19 carbon alkyl chains,[25, 27] and $[Ru(bpy)(4,4'\text{-}R_2bpy)_2]^{2+}$, where R is heptadecyl alkyl.[22] The first type of ruthenium complexes forms spherical micelles in water with headgroup areas around 100 $Å^2$, as shown by small-angle neutron scattering. The second type of ruthenium complexes yields spherical inverted micelles and spherical inverted vesicles in hexane and toluene, respectively.[22] It should be noted that the molecular structure of this latter complex is more comparable to the present complexes, since the number of alkyl chains per molecule is in both cases 4, whereas for complexes $[Ru(bpy)_2(4,4'\text{-}R_2bpy)]^{2+}$ the number of alkyl chains is 2. The difference in number of alkyl chains, and thus in the volume of the hydrophobic moiety, is expected to strongly influence the type of aggregate that is formed, based on the geometrical considerations proposed by Israelachvili[37] for surfactant self-assembly. Since for the present compounds the number of alkyl chains is 4, but the number of carbon atoms in these chains is lower than for the ruthenium complexes, the packing parameter should be intermediate between those of $[Ru(bpy)_2(4,4'\text{-}R_2bpy)]^{2+}$ and $[Ru(bpy)(4,4'\text{-}R_2bpy)_2]^{2+}$, *i.e.* in the range expected for bilayer formation.

The size exclusion experiments with the fluorescent probe show that in all cases the aggregates contain encapsulated solvent, and the AFM results indicate that extensive drying of the samples results in flattened structures. The presence of a solvent core is

not apparent from the TEM images, but it is not expected to be detected there because of the strong scattering of the electrons by the metal ions in the surfactants. Thus it seems that water is present inside the aggregates, which is important in order to keep their spherical or rod-like morphology. The 2.6 nm plateau that surrounds the collapsed aggregates of compound **4** has a mean thickness commensurate with that expected for a bilayer structure (as based on a simple CPK model that predicts an extended length of 1.7 nm for this compound). The difference between the measured value (2.6 nm) and the theoretical bilayer thickness (3.4 nm) may imply some interdigitation or tilting of the molecules in the bilayer. We undertook powder X-ray diffraction studies on the dried material, expecting not only to obtain further evidence for the formation of bilayers, but also to determine the bilayer thicknesses and relate them to the molecular structures. Unfortunately, the diffraction patterns showed only weak and broad peaks indicating a large disorder in the aggregated state; no set of peaks that could be assigned to a lamellar packing of stacked bilayers was observed. The failure to detect any lamellar packing suggests that compounds **1**-**5** do not have a large tendency to form regular stacked bilayers; this is in line with the observation of material with a thickness corresponding to only one single bilayer in the AFM experiment of compound **4**. As bilayer thicknesses could not be obtained it was not possible to draw any conclusions with respect to the effect of the number and length of the alkyl tails on the molecular packing of the compounds.

In the AFM experiments we were able to study the effect of dehydration on the structure of the aggregates. Since the TEM and SEM pictures were taken under high vacuum, we could not perform such experiments. Nevertheless, the intriguing question remains, why the TEM and SEM images more closely resemble the AFM images of hydrated vesicles, than those of the dehydrated vesicles. That is, why were the vesicles

as observed by SEM and TEM not surrounded by the material seen in the AFM images of dehydrated vesicles? One possible explanation is that the present compounds have a higher affinity for the support used in the AFM studies (mica) than for the support used in TEM and SEM studies (formvar and glass, respectively).

Another important experimental observation requiring an explanation is the unusual rod-like vesicle aggregation observed for the short chain amphiphiles **1**, **2**, and **3**. Self-assembly into tubules, rods and fibers is usually restricted to cases where the driving force for assembly is some directional intermolecular interaction, such as hydrogen bonding, and π-π stacking.[38-43] Although for compounds **1**-**5** the existence of π-π stacking between bipyridine ligands on neighboring molecules may not be ruled out completely, the *cis* configuration around the metal center and the steric hindrance of the alkyl groups at the positions 4 and 4' of these ligands make this type of interaction very unlikely. In addition, a question that remains open is why the directional interaction between molecules is not expressed in the case of the aggregates of the compounds with longer alkyl chains, *i.e.* compounds **4** and **5**. The formation of rod-like vesicles may be related to the molecular structure imposed by the coordination center. In the most extended conformation of the alkyl chains, the overall shape of the molecules of this type of compounds resembles a see-saw or an octahedral molecule with two adjacent positions much shorter (cyanides) than the other four, as schematically represented in Fig. 6. This shape creates void spaces that may be occupied by the alkyl chains of a neighbor molecule either in the same or in an opposite monolayer. As may be seen in Fig. 6, the molecules are also very asymmetric in shape, and this asymmetry may lead to a preference for an elongated aggregate structure. Anisotropic aggregation induced by an anisotropic shape of the molecule has been described for gemini surfactants.[44, 45] As the length of the alkyl chain increases this effect may be reduced because the longer

chains may occupy the void space more effectively, and thus make the molecular shape more symmetric.

The results obtained of the experiments at different aggregation times show that all aggregates have a strong tendency to fuse into larger structures. This behavior is typical of neutral surfactants, but the presence of four alkyl chains per molecule may also play a role. In fact, simulation studies on the aggregation behavior of single- and double-tail surfactants indicate that, by increasing the number of lipophilic tails, the ability of the headgroup to shield the hydrophobic tails from the solvent becomes weaker.[46] This inability to shield the tails introduces some disorder in the molecular aggregates because the solvent becomes inserted into the lipid cores, increasing the driving force for aggregation/fusion.

The behavior of the aggregates upon addition of increasing concentrations of methanol is also typical of amphiphilic compounds. It is well known from experimental and computational studies that the addition of methanol to amphiphilic aggregates decreases the bilayer thickness because it induces interdigitation of the tails, and hence fusion events.[47]. These effects have been attributed to the fact that the alcohol molecules become located at the hydrophilic/hydrophobic interface, which increases the average headgroup area, and to a decrease of the interfacial tension as a result of the increase in alcohol concentration in the bulk solvent.

Taken together, our results suggest that self-assembly of the compounds **1**-**5** is a kinetically driven process, and that the thermodynamically stable morphology of the aggregates in all cases is the bilayer structures observed in aged samples, either in the form of large vesicles and rod-like structures or as films.

Conclusion

This study reports on the aggregation behavior of metallosurfactants derived from iron(II) complexes with lipophilic bipyridine ligands. The morphological characterization was performed by several microscopic techniques, namely SEM, cryo-SEM, TEM and AFM, and the results obtained show that in all cases the morphology of the aggregates greatly depends on the length of the alkyl chains attached to the bipyridine ligand. For shorter alkyl chains rod-like nanostructures were observed, whereas for longer alkyl chains only spherical nanostructures were found. The formation of aggregates of these complexes is noteworthy because they contain relatively short alkyl chains allowing only weak hydrophobic interactions between the lipophilic chains. The fact that aggregation nonetheless occurs, indicates that other interactions, in particular those involving the hydrophobic bipyridine ligands, or solvent-mediated hydrogen bonding between cyanide ligands from neighboring complex molecules, are also important. Nevertheless, it is likely that the poor hydrophobic interaction between the chains and the asymmetry of the molecular structure of the complexes with short alkyl tails determine the final relative orientation of the adjacent molecules in the aggregate. Increase of the alkyl chain attenuates this asymmetry effect, possibly because the space between the molecules becomes better filled, while interdigitation of lipophilic tails may also play a role. Further studies on the packing of the compounds are being carried out in order to elucidate this behavior.

Study of the effects of dehydration of the vesicles suggests that water is important for retaining the vesicle structure. It furthermore suggests that the internal structure of the vesicles is made up of (possibly concentric) bilayers of molecules.

In comparison with other amphiphilic metal bipyridine complexes reported so far in the literature, the present complexes exhibit a higher tendency to form bilayer structures that enclose an aqueous compartment. This stabilization of bilayer structures is probably

due to the higher number of alkyl chains per molecule. The present compounds are thus promising candidates for the preparation of bilayer structures containing metal complexes, and to introduce metal complex reactivity and special physical properties in soft-materials.

Acknowledgments

We thank Fundação para a Ciência e Tecnologia (FCT) for financial support through Contract nr. POCTI/QUI/38605/2001. P. Garcia thanks FCT for grant PRAXIS XXI/BD/15922/98. P. Eaton thanks FCT for grant SFRH/BPD/17617/2004. We thank Laboratório de Química Analítica, Faculdade de Ciências, Universidade do Porto for the use of the AFM microscope.

Scheme 1. Chemical structure of the compounds studied: compound **1**: m=n=5; compound **2**: m=n=7; compound **3**: m=7, n=1; compound **4**: m=n=9, compound **5**: m=n=13.

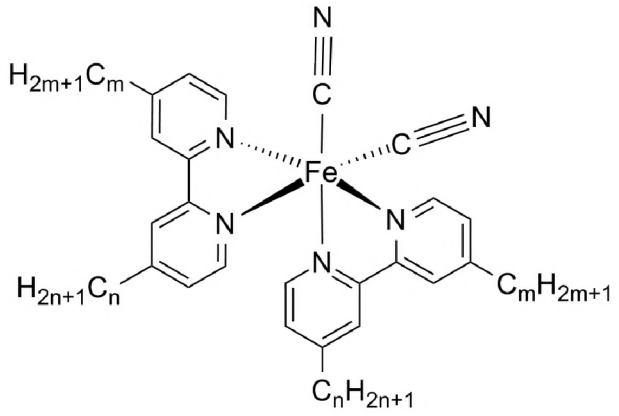

.

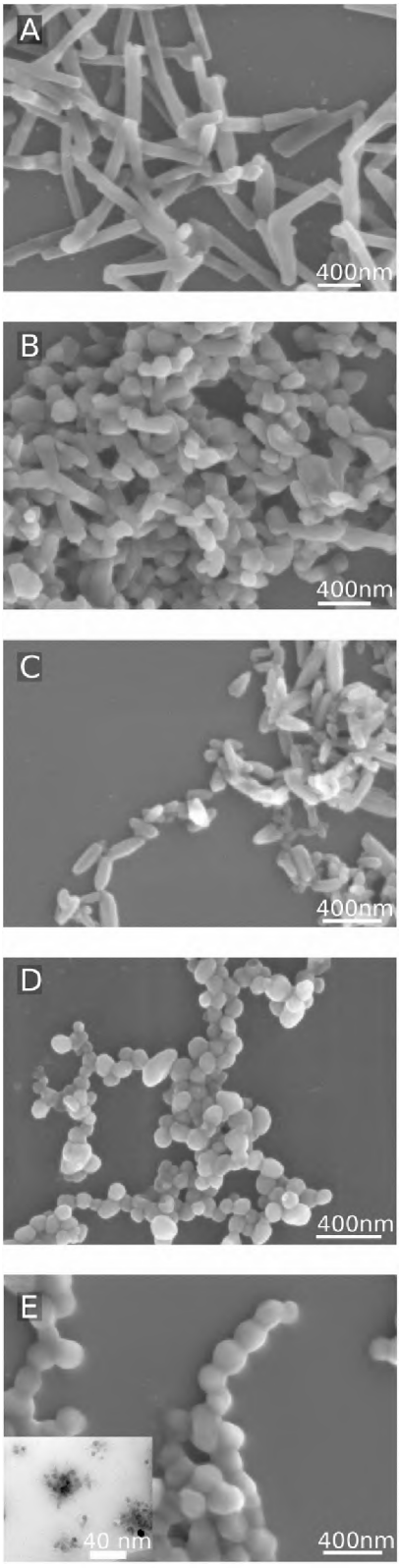

Figure 1. SEM micrographs of freshly prepared samples of compounds **1** (A), compound **2** (B) compound **3** (C), compound **4** (D) and compound **5** (E). The inset of E is a higher magnification image showing the smaller features observed in this sample.

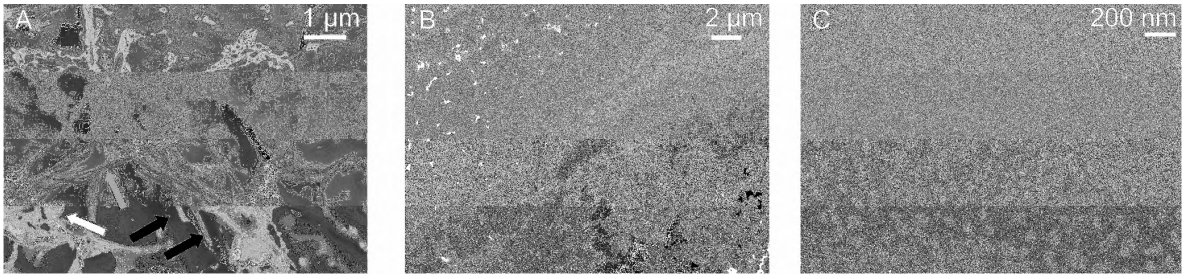

Figure 2. Cryo-SEM micrographs of freshly prepared samples of compounds **1** (A), compound **2** (B), and compound **4** (C). For the meaning of the arrows, see text.

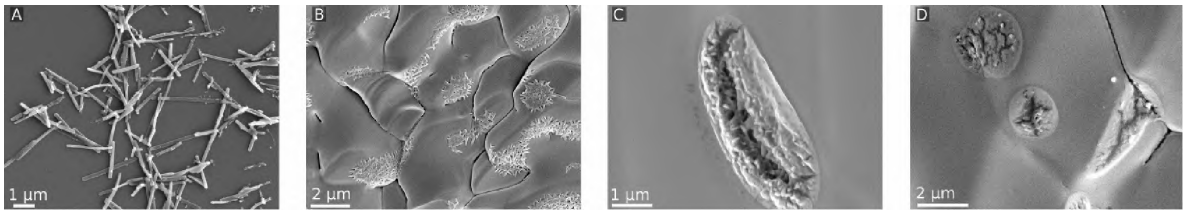

Figure 3. (A) SEM image of a sample of compound **1** after 1 day in solution; (B) and (C) cryo-SEM micrographs of a sample of compound **2** after 9 days in solution; (D) cryo-SEM micrograph of a sample of compound **4**, after 9 days in solution.

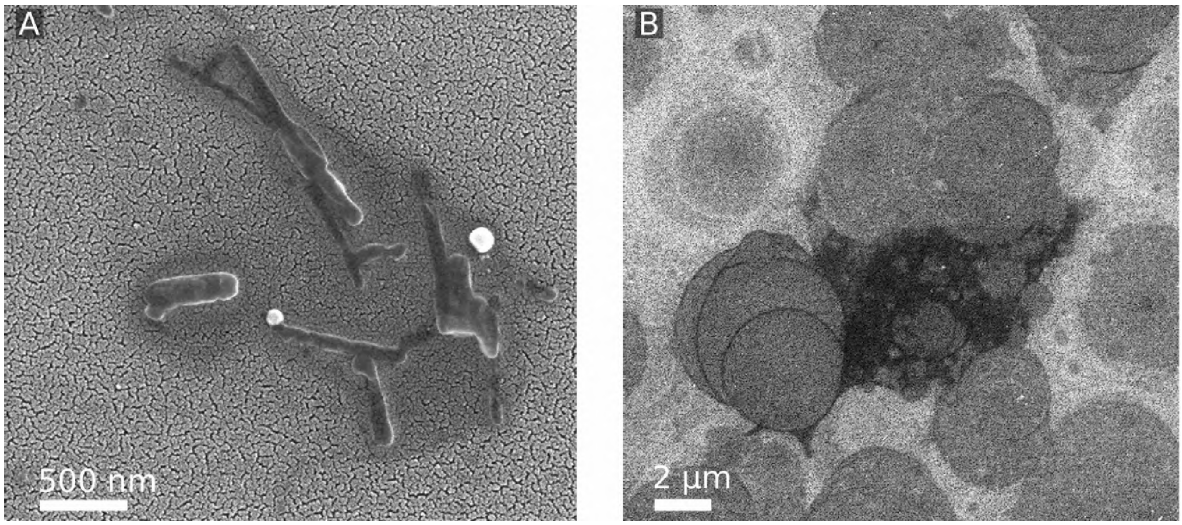

Figure 4. SEM micrographs of samples of (A) compound **1** with addition of 5% (v:v) methanol; and (B) compound **4** with addition of 75% (v:v) methanol.

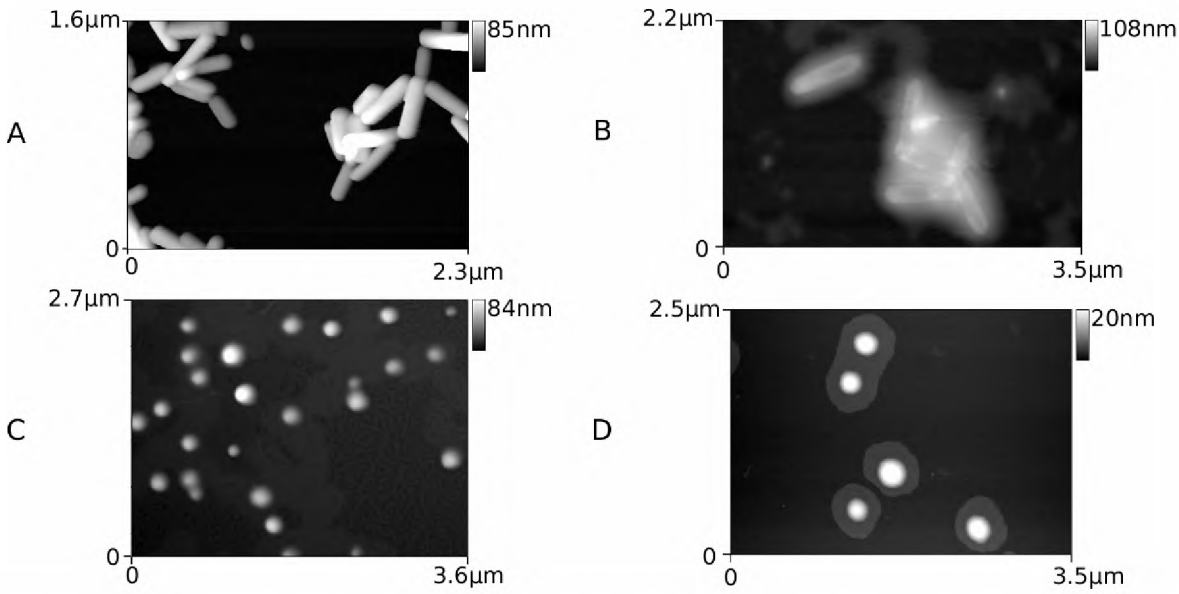

Figure 5. AFM images of vesicles formed from compound **1** imaged after air drying on the mica substrate (A), and after vacuum drying (B) and compound **4** imaged after drying in air(C) and under vacuum (D)

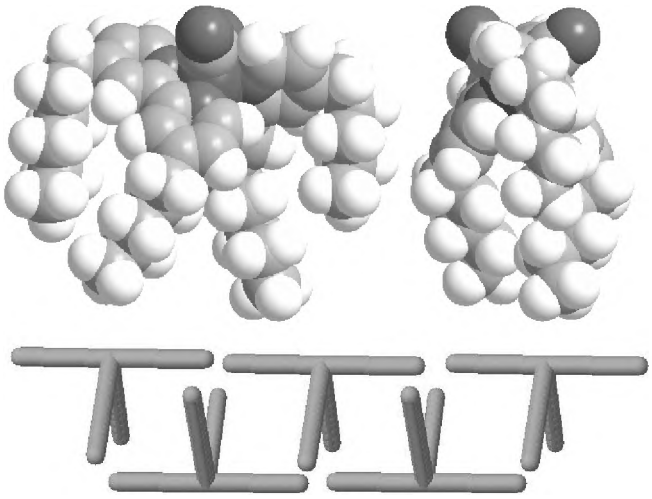

Figure 6: (A) Side views of the molecular structure of compound 1 obtained by minimization of steric energy (MM2 Chem3D 10.0). (B) Schematic representation of possible molecular aggregation.

Compound 1	**Compound 4**

	Length / nm	Width / nm	Aspect Ratio	Width / nm
AFM	380-700	60-80	6.0-9.0	40-55
TEM	660-940	70-125	5.0-10.0	50-100
SEM	1200-1700	120-150	9.0-12.0	80-130

Table 1: Average vesicle dimensions as measured by AFM, TEM and SEM, values are the range of averages for different batches (at least 20 measurements per batch). Widths as reported from AFM measurements were measured from vesicle heights (see text).

References

1. Binnemans, K.; Gorller-Walrand, C., Lanthanide-containing liquid crystals and surfactants. *Chemical Reviews* **2002,** 102, (6), 2303-2345.
2. Jervis, H. B.; Raimondi, M. E.; Raja, R.; Maschmeyer, T.; Seddon, J. M.; Bruce, D. W., Templating mesoporous silicates on surfactant ruthenium complexes: a direct approach to heterogeneous catalysts. *Chemical Communications* **1999**, (20), 2031-2032.
3. Danks, M. J.; Jervis, H. B.; Nowotny, M.; Zhou, W. Z.; Maschmeyer, T. A.; Bruce, D. W., High-activity heterogeneous catalysts prepared in one step from the mesophases of metallosurfactants. *Catalysis Letters* **2002,** 82, (1-2), 95-98.
4. Donnio, B., Lyotropic metallomesogens. *Current Opinion in Colloid & Interface Science* **2002,** 7, (5-6), 371-394.
5. Serrano, J. L.; Sierra, T., Helical supramolecular organizations from metal-organic liquid crystals. *Coordination Chemistry Reviews* **2003,** 242, (1-2), 73-85.
6. Nazeeruddin, M. K.; Zakeeruddin, S. M.; Lagref, J. J.; Liska, P.; Comte, P.; Barolo, C.; Viscardi, G.; Schenk, K.; Graetzel, M., Stepwise assembly of amphiphilic ruthenium sensitizers and their applications in dye-sensitized solar cell. *Coordination Chemistry Reviews* **2004,** 248, (13-14), 1317-1328.
7. Chu, B. W. K.; Yam, V. W. W., Synthesis, characterization, Langmuir-Blodgett film-forming properties, and second-harmonic-generation studies of ruthenium(II) complexes with long hydrocarbon chains. *Inorganic Chemistry* **2001,** 40, (14), 3324-3329.
8. Tse, C. W.; Lam, L. S. M.; Man, K. Y. K.; Wong, W. T.; Chan, W. K., Svnthesis and characterization of random and block copolymers with pendant rhenium diimine complexes by controlled radical polymerization. *Journal of Polymer Science Part a-Polymer Chemistry* **2005,** 43, (6), 1292-1308.
9. Romualdo-Torres, G.; Agricole, B.; Mingotaud, C.; Ravaine, S.; Delhaes, P., Hybrid organic-inorganic Langmuir-Blodgett films starting from colloidal Prussian Blue solution. *Langmuir* **2003,** 19, (11), 4688-4693.
10. Terasaki, N.; Akiyama, T.; Yamada, S., Structural characterization and photoelectrochemical properties of the self-assembled monolayers of Tris(2(')2 '-

bipyridine)ruthenium(II)-viologen linked compounds formed on the gold surface. *Langmuir* **2002,** 18, (22), 8666-8671.
11. Qiu, L. G.; Xie, A. J.; Shen, Y. H., Metallomicellar catalysis: Hydrolysis of p-nitrophenyl picolinate catalyzed by Cu(II) complexes of triazole-based ligands in cationic gemini surfactant micelles. *Journal of Molecular Catalysis A-Chemical* **2006,** 244, (1-2), 58-63.
12. Bhattacharya, S.; Snehalatha, K.; Kumar, V. P., Synthesis of new Cu(II)-chelating ligand amphiphiles and their esterolytic properties in cationic micelles. *Journal of Organic Chemistry* **2003,** 68, (7), 2741-2747.
13. Jiang, F.; Jiang, B. Y.; Cao, Y. S.; Meng, X. G.; Yu, X. Q.; Zeng, X. C., Metallomicellar catalysis - Hydrolysis of phosphate monoester by Cu(II), Zn(II), Ni(II) and Co(II) complexes of pyridyl ligands in CTAB micellar solution. *Colloids and Surfaces a-Physicochemical and Engineering Aspects* **2005,** 254, (1-3), 91-97.
14. Walker, G. W.; Geue, R. J.; Sargeson, A. M.; Behm, C. A., Surface-active cobalt cage complexes: synthesis, surface chemistry, biological activity, and redox properties. *Dalton Transactions* **2003**, (15), 2992-3001.
15. Luo, X. Z.; Miao, W. G.; Wu, S. X.; Liang, Y. Q., Spontaneous formation of vesicles from octadecylamine in dilute aqueous solution induced by Ag(I) ion. *Langmuir* **2002,** 18, (24), 9611-9612.
16. Wang, J. Z.; Song, A. X.; Jia, X. F.; Hao, J. C.; Liu, W. M.; Hoffmann, H., Two routes to vesicle formation: Metal-ligand complexation and ionic interactions. *Journal of Physical Chemistry B* **2005,** 109, (22), 11126-11134.
17. Blasini, D. R.; Flores-Torres, S.; Smilgies, D. M.; Abruna, H. D., Stepwise self-assembly of ordered supramolecular assemblies based on coordination chemistry. *Langmuir* **2006,** 22, (5), 2082-2089.
18. Holder, E.; Marin, V.; Alexeev, A.; Schubert, U. S., Greenish-yellow-, yellow-, and orange-light-emitting iridium(III) polypyridyl complexes with poly (epsilon-capro lactone)-bipyridine macroligands. *Journal of Polymer Science Part a-Polymer Chemistry* **2005,** 43, (13), 2765-2776.
19. Garcia, P.; Marques, J.; Pereira, E.; Gameiro, P.; Salema, R.; de Castro, B., A novel self-indicative vesicle based on a iron(II) complex. *Chemical Communications* **2001**, (14), 1298-1299.
20. Tollner, K.; PopovitzBiro, R.; Lahav, M.; Milstein, D., Impact of molecular order in Langmuir-Blodgett films on catalysis. *Science* **1997,** 278, (5346), 2100-2102.
21. Soyer, H.; Mingotaud, C.; Boillot, M. L.; Delhaes, P., Spin crossover of a Langmuir-Blodgett film based on an amphiphilic iron(II) complex. *Langmuir* **1998,** 14, (20), 5890-5895.
22. Dominguez-Gutierrez, D.; Surtchev, M.; Eiser, E.; Elsevier, C. J., Ru(II)-based metallosurfactant inverted aggregates. *Nano Letters* **2006,** 6, (2), 145-147.
23. Kobayashi, K.; Sato, H.; Kishi, S.; Kato, M.; Ishizaka, S.; Kitamura, N.; Yamagishi, A., Spectroscopic evidence for Pt-Pt interaction in a Langmuir-Blodgett film of an amphiphilic platinum(II) complex. *Journal of Physical Chemistry B* **2004,** 108, (48), 18665-18669.
24. Taniguchi, M.; Ueno, N.; Okamoto, K.; Karthaus, O.; Shimomura, M.; Yamagishi, A., Monolayer and fluorescence properties of a chiral amphiphilic ruthenium(II) complex at an air-water interface. *Langmuir* **1999,** 15, (22), 7700-7707.
25. Bowers, J.; Amos, K. E.; Bruce, D. W.; Heenan, R. K., Surface and aggregation behavior of aqueous solutions of Ru(II) metallosurfactants: 4. Effect of chain number and orientation on the aggregation of [Ru(bipy)(2)(bipy ']Cl-2 complexes. *Langmuir* **2005,** 21, (13), 5696-5706.

26. Bowers, J.; Amos, K. E.; Bruce, D. W.; Webster, J. R. P., Surface and aggregation behavior of aqueous solutions of Ru(II) metallosurfactants. 3. Effect of chain number and orientation on the structure of adsorbed films of [Ru(bipy)(2)(bipy ')]Cl-2 complexes. *Langmuir* **2005,** 21, (4), 1346-1353.
27. Bowers, J.; Danks, M. J.; Bruce, D. W., Surface and aggregation behavior of aqueous solutions of Ru(II) metallosurfactants: 1. Micellization of [Ru(bipy)(2)(bipy ')][Cl](2) complexes. *Langmuir* **2003,** 19, (2), 292-298.
28. Bowers, J.; Danks, M. J.; Bruce, D. W.; Webster, J. R. P., Surface and aggregation behavior of aqueous solutions of Ru(II) metallosurfactants: 2. Adsorbed films of [Ru(biPY)(2)(bipy ')][Cl](2) complexes. *Langmuir* **2003,** 19, (2), 299-305.
29. Gameiro, P.; Pereira, E.; Garcia, P.; Breia, S.; Burgess, J.; de Castro, B., Derivatives of bis(2,2 '-bipyridyl)dicyanoiron(II) with long alkyl chains - Versatile solvatochromic probes that form metalloaggregates in water-rich media. *European Journal of Inorganic Chemistry* **2001**, (11), 2755-2761.
30. Pereira, E.; Garcia, P.; Breia, S.; Maia, A.; Gameiro, P.; de Castro, B., Solvatochromic iron(II) complexes as polarity probes for micellar media. *Biophysical Journal* **2001,** 80, (1), 374a-374a.
31. Schilt, A. A., Mixed Ligand Complexes of Iron(Ii) and Iron(Iii) with Cyanide and Aromatic Di-Imines. *Journal of the American Chemical Society* **1960,** 82, (12), 3000-3005.
32. Cuccovia, I. M.; Schroter, E. H.; Baptista, R. C. D.; Chaimovich, H., Effect of Detergents on S-Acyl to N-Acyl Transfer of S-Acyl-Beta-Mercaptoethylamines. *Journal of Organic Chemistry* **1977,** 42, (21), 3400-3403.
33. New, R. R. C., *Liposomes – A practical approach*. Oxford University: Oxford, 1990.
34. B Jönsson, B. L., K. Holmberg, B Kronberg, *Surfactants and Polymers in Aqueous Solution*. John Wiley and Sons: New York, 1998.
35. Gibson, C. T.; Watson, G. S.; Myhra, S., *Scanning* **1997,** 19, (8), 564-581.
36. Oszwaldowski, S.; Marchut, D., Characterization of iron(II)(alpha-diimine) chelates and their interactions with anionic, cationic and non-ionic micelles using the separation, spectrophotometric and computational methods. *Analytica Chimica Acta* **2005,** 540, (1), 207-219.
37. Israelachvili, J. N.; Mitchell, D. J.; Ninham, B. W., Theory of Self-Assembly of Hydrocarbon Amphiphiles into Micelles and Bilayers. *Journal of the Chemical Society-Faraday Transactions Ii* **1976,** 72, 1525-1568.
38. Sommerdijk, N. A. J. M.; Buynsters, P. J. A. A.; Pistorius, A. M. A.; Wang, M.; Feiters, M. C.; Nolte, R. J. M.; Zwanenburg, B., Tuning the Supramolecular Expression of Chirality - Phospholipid Analogs Containing Amide Linkages. *Journal of the Chemical Society-Chemical Communications* **1994**, (17), 1941-1942.
39. Sommerdijk, N. A. J. M.; Feiters, M. C.; Nolte, R. J. M.; Zwanenburg, B., Aggregation Behavior of a Phospholipid Based on D-(-)-Threitol. *Recueil Des Travaux Chimiques Des Pays-Bas-Journal of the Royal Netherlands Chemical Society* **1994,** 113, (4), 194-200.
40. Sommerdijk, N. A. J. M.; Lambermon, M. H. L.; Feiters, M. C.; Nolte, R. J. M.; Zwanenburg, B., Boomerang shaped aggregates from a histidine surfactant. *Chemical Communications* **1997**, (5), 455-456.
41. Fuhrhop, J. H.; Helfrich, W., Fluid and Solid Fibers Made of Lipid Molecular Bilayers. *Chemical Reviews* **1993,** 93, (4), 1565-1582.

42. Boettcher, C.; Schade, B.; Fuhrhop, J. H., Comparative cryo-electron microscopy of noncovalent N-dodecanoyl- (D- and L-) serine assemblies in vitreous toluene and water. *Langmuir* **2001,** 17, (3), 873-877.
43. Fuhrhop, J. H.; Schnieder, P.; Boekema, E.; Helfrich, W., Lipid Bilayer Fibers from Diastereomeric and Enantiomeric N-Octylaldonamides. *Journal of the American Chemical Society* **1988,** 110, (9), 2861-2867.
44. Oda, R.; Huc, I.; Homo, J. C.; Heinrich, B.; Schmutz, M.; Candau, S., Elongated aggregates formed by cationic gemini surfactants. *Langmuir* **1999,** 15, (7), 2384-2390.
45. Oda, R.; Laguerre, M.; Huc, I.; Desbat, B., Molecular organization of gemini surfactants in cylindrical micelles: An infrared dichroism spectroscopy and molecular dynamics study. *Langmuir* **2002,** 18, (25), 9659-9667.
46. Shillcock, J. C.; Lipowsky, R., Equilibrium structure and lateral stress distribution of amphiphilic bilayers from dissipative particle dynamics simulations. *Journal of Chemical Physics* **2002,** 117, (10), 5048-5061.
47. Patra, M.; Salonen, E.; Terama, E.; Vattulainen, I.; Faller, R.; Lee, B. W.; Holopainen, J.; Karttunen, M., Under the influence of alcohol: The effect of ethanol and methanol on lipid bilayers. *Biophysical Journal* **2006,** 90, (4), 1121-1135.

TOC GRAPHIC